# The Mechanics of Large Gas Bubbles in Tubes

## I. Bubble Velocities in Stagnant Liquids

*R. A. S. BROWN*

*Department of Chemical and Petroleum Engineering, University of Alberta, Edmonton, Alta.*

**The effect of liquid viscosity on the rate of rise of a large gas bubble through stagnant liquid in a tube is shown to be limited to that on the film flow past the bubble on the wall of the tube. A criterion of similarity between the shapes of bubbles in different liquids is obtained experimentally which enables development of a correlation for the velocities of rise. This correlation is shown to be in good agreement with experimental results for systems in which the effects of surface tension and liquid viscosity on the frontal flow are negligible.**

**On démontre que l'effet de la viscosité de la phase continue sur le taux d'ascension d'une bulle de gaz dans un liquide stagnant, dans un tube, est limité à l'effet de l'écoulement du film sur la paroi du tube auprès de la bulle. Un critère de similitude entre la géométrie des bulles dans divers liquides est obtenu expérimentalement, ce qui permet le développement d'une corrélation pour les vitesses d'ascension. Cette corrélation est en accord avec les résultats expérimentaux pour les systèmes dans lesquels les effets de tension superficielle et de viscosité du liquide sur l'écoulement frontal sont négligeables.**

In the concurrent, upwards flow of gas-liquid mixtures in vertical pipes, one of the stable geometries encountered is that of large, bullet-shaped bubbles of gas which rise through the liquid. This study, which is concerned with the description of the behavior of single large bubbles in stagnant liquids, is part of a broader investigation of bubble behavior in gas-liquid slug flow, the ultimate aim being to improve the prediction of pressure drops in two-phase flow through a better understanding of the mechanics of flow. The extension of this analysis of bubble mechanics to slug flow is made in Part II.

Since the main purpose of this study of single bubble movement was to obtain information which could be used eventually in the analysis of slug flow, consideration was limited to bubbles large in diameter relative to the tube. In addition, systems for which the viscosity or surface tension was sufficiently large to affect the frontal flow were considered only to the extent of defining the limits of the correlation developed.

## THE MOVEMENT OF LARGE BUBBLES IN TUBES

Previous studies by Griffith and Wallis[1]* and by Nicklin[2] have also used the study of bubbles rising through stagnant liquids as a starting point for two-phase flow studies. This is quite understandable since the geometries of gas bubbles encountered in the slug flow region are similar to those of bubbles rising in stagnant liquids. These bubbles exhibit a blunt near-spherical nose followed by a tapered transition region and a cylindrical tail. For short bubbles, the bubble profile may not be sufficiently developed to have the cylindrical portion.

The cavity formed in a tube filled with liquid when the liquid is allowed to drain from the bottom of the tube has this same characteristic shape and it has been shown[2] that the rate of rise of the cavity is the same as the velocity of a finite bubble in the tube. These large bubbles will be referred to as Taylor bubbles following an earlier suggestion in the literature[1]. A photograph of a Taylor bubble is shown in Figure 1.

**Figure 1—Photograph of a Taylor bubble.**

### *Bubble Characteristics in Inviscid Liquids*

Dumitrescu[3] and Davies and Taylor[4] proposed that the behavior of bubbles rising through actual liquids in tubes could be approximated by the hypothetical case of a bubble rising through an inviscid liquid. This assumption reduces the problem to that of determining the shape of cavity and the velocity of rise under potential flow conditions. The physical situation has been illustrated in Figure 2 where, for convenience, the liquid is shown approaching the stationary bubble with a velocity $V_b^o$.†

*Present address: Coal Research Division, Research Council of Alberta, Edmonton, Alta.*

*Reference citations for the two papers have been combined and are given at the end of Part II.

†Nomenclature for this paper and for Part II is defined at the end of Part II.

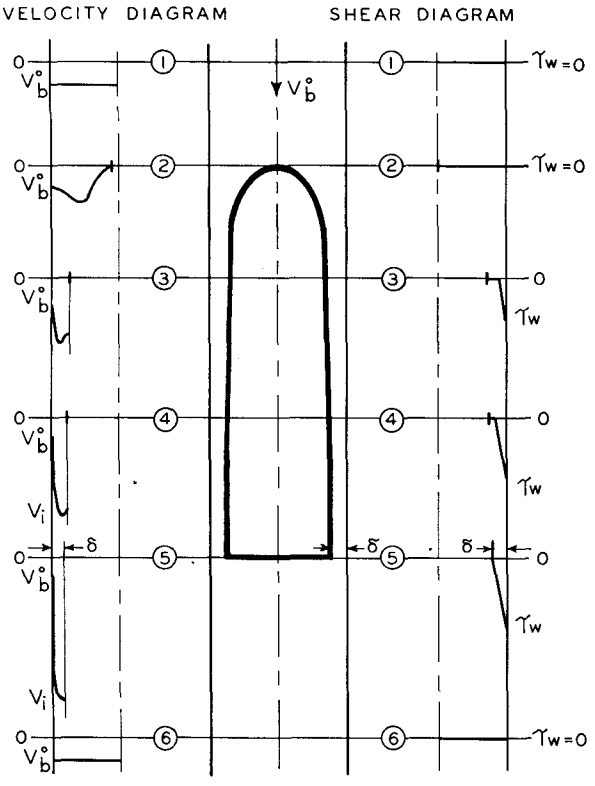


**Figure 2—Proposed model of a Taylor bubble.**

Since gas-liquid systems are being considered, the density of the bubble fluid can be neglected relative to the density of the liquid and the surface of the bubble is therefore a surface of constant pressure. Applying Bernoulli's equation to a streamline in the interface gives

$$V_i^2 = 2g(-z) \quad \ldots\ldots(1)$$

where $V_i$ is the tangential velocity at the interface at a vertical distance of $(-z)$ below the stagnation point. The difficulty in solving the problem arises because the coordinates of the surface on which Equation (1) is to be satisfied are not known and must also be determined by the solution.

Dumitrescu obtained the potential function for the flow in a tube, assumed that the bubble would have a spherical nose and solved simultaneously the flow around the spherical nose and the asymptotic film flow to obtain the bubble velocity and the frontal radius of curvature. The asymptotic film profile was obtained by assuming plug flow in the film and writing the material balance equation

$$V_b^o R^2 = \sqrt{2g(-z)}\,(R^2 - r_i^2) \quad \ldots\ldots(2)$$

The simultaneous solution of the flows at the nose and in the film gave the results

$$V_b^o = 0.496\sqrt{gR} \quad \ldots\ldots(3)$$

and

$$r_o = 0.75R \quad \ldots\ldots(4)$$

and the two solutions joined at the point $-z = 0.50R$, $r_i = 0.71R$.

Davies and Taylor[4] also obtained the potential function for flow in a tube as did Dumitrescu, but chose to solve the flow by truncating the resulting equations and satisfying Equation (1) and the stream function at the stagnation point and one arbitrary point which was chosen as the mid-radial position. This procedure led to the relation

$$V_b^o = 0.464\sqrt{gR} \quad \ldots\ldots(5)$$

Both of these theoretical solutions are approximate and have a number of shortcomings. Equation (2), which was used by Dumitrescu to describe the film flow, assumes that the radial component of velocity is negligible and that the momentum flux at the section $z = 0$ is negligible relative to the momentum flux in the film. Both of these assumptions are questionable at the point of tangency which was obtained. With respect to Davies and Taylor's solution, the approximations inherent in truncating the solution are apparent and the authors noted that the solution was only a first approximation to the correct one. Nicklin[2] showed that the solution was not unique and was quite dependent on the choice of the arbitrary point. As this point was chosen closer to the stagnation point, the solution tended to the limiting value

$$V_b^o = 0.503\sqrt{gR} \quad \ldots\ldots(6)$$

Despite the approximations made in obtaining these solutions, they come surprisingly close to predicting the velocities of air bubbles rising in liquids of low viscosities which would be expected to behave most like the inviscid case. Equation (3) is significantly better than Equation (5) due to the less severe truncation of the series equations arising in the solutions.

### *Bubble Characteristics in Actual Liquids*

**General Considerations—Proposed Model:** Entirely apart from the foregoing discussion of the accuracy of the solutions based on potential flow theory, there is the question of how well these solutions can be expected to apply when air bubbles rising through liquids of higher viscosity are considered and the hypothesis of potential flow becomes questionable. To obtain an indication of the effect of deviation from the potential flow situation, a series of velocity determinations were made

TABLE 1
EXPERIMENTAL BUBBLE VELOCITIES

| Liquid | Density lb./ft.$^3$ | Viscosity cp | Surface Tension dyne/cm. | Bubble Velocity $V_b^o$, ft./sec. | $\frac{V_b^o}{\sqrt{gR}}$ | $\delta_o$[a] inches | $\frac{V_b^o}{\sqrt{g(R-\delta_o)}}$ |
|---|---|---|---|---|---|---|---|
| | (1) | (2) | (3) | (4) | (5) | (6) | (7) |
| Water[b] | 62.3 | 0.977 | 72.7 | 0.577 | 0.489 | 0.0272 | 0.502 |
| Varsol[b] | 49.1 | 0.942 | 24.4 | 0.571 | 0.484 | 0.0290 | 0.498 |
| Marcol[b] | 54.0 | 19.42 | 29.5 | 0.558 | 0.472 | 0.0733 | 0.510 |
| Primol[b] | 55.0 | 142.3 | 30.5 | 0.494 | 0.418 | 0.1302 | 0.484 |
| — Dumitrescu (Equation (3)) | | | | | 0.496 | | |
| — Davies and Taylor | | | | | | | |
| — (Equation (5)) | | | | | 0.464 | | |
| — (Equation (6)) | | | | | 0.503 | | |

[a]Calculated from the bubble velocity with Equation (10)
[b]Tube Radius = 0.519 inch.

for air bubbles rising in liquids of different viscosities contained in a 1.038-in. diameter tube. The properties of the liquids used in these experiments are given in Table 1 while the details of the experimental equipment and procedures used are included as Appendix I.

The results of the velocity determinations for these bubbles are given also in Table 1 (columns 4 and 5) along with the predictions of bubble velocities in inviscid liquids obtained from Equations (3), (5) and (6). These results indicate that the potential flow solution given by Equation (3), while describing the velocities of bubbles in liquids of low viscosity quite well, is not suitable when liquids having higher viscosities are considered.

As the divergence of the experimental results from the solution for inviscid liquids was not too marked, it was decided to attempt to modify the potential flow solution to account for the effect of liquid viscosity. This approach seemed feasible as the flow around the bubble on the tube wall would be affected by the viscosity of the liquid while the flow at the nose might remain independent of liquid viscosity even for reasonably high viscosities due to the flat velocity profile in the approach flow. The proposed model is shown in Figure 2 and is explained in the following paragraphs.

The model shown in Figure 2 differs from the potential flow model in the flow on the wall of the tube past the bubble where a developing boundary layer is superposed on the potential flow. The development of this laminar film flow is shown in idealized form in the diagrams of shear stress and velocity distributions which are included with Figure 2. In the coordinate system used, in which velocities relative to the bubble are considered, the liquid approaching the bubble at a distance from the nose (i.e., section 1) is in true plug flow and there are no velocity gradients. At the nose of the bubble, section 2, the presence of the stagnation point has modified the velocity distribution but this deformation is due primarily to the pressure field and little or no formation of the laminar boundary layer has occurred. Two intermediate stages in the formation of the boundary layer are shown at sections 3 and 4 where, as the liquid in the film accelerates, successively more is influenced by the shear flow on the wall and the laminar layer becomes thicker. At the tail of the bubble, section 5, the laminar layer is assumed to be fully developed. In this region the film is entirely supported by the wall shear stress. For long bubbles, the length of this fully developed laminar film flow might be a significant proportion of the total bubble length. At positions sufficiently far behind the bubble, plug flow occurs once more as shown for section 6.

While this model presents a greatly idealized representation of the actual liquid flow, it does account for the effect of liquid viscosity in the film flow and constitutes an improvement over the inviscid liquid model. The liquid flow in the film and nose regions will next be considered in more detail with a view to solving the over-all flow situation.

**The Film Region:** The assumption of potential flow in the film for large $-z$, as developed by Dumitrescu[3], led to Equation (2) which can be rewritten in terms of the film thickness,

$$\delta_o = R - r_i \qquad (7)$$

to obtain

$$\xi_o = \frac{V_b^o}{\sqrt{8gR\eta}} \qquad (8)$$

where the relative film thickness, $\delta_o/R$, has been denoted by $\xi_o$ and the axial coordinate, $-z/R$, by $\eta$. In Equation (8), the film thickness has been assumed small and $\xi_o^2$ neglected. Equation (8) can be tested for actual systems by experimental observation of the variation of film thickness along the bubble. This has been done both by Davies and Taylor[4] for air bubbles rising through water in a 3.13-in. diameter tube and by Goldsmith and Mason[5] for air bubbles rising through a silicone oil (viscosity = 5.6 centipoise) in a 0.197-in. diameter tube. Despite the fact that the observed bubble velocities were quite well represented by Equation (3) in each case, Davies and Taylor's film measurements indicated a thickness about 30% greater than predicted by Equation (8) while Goldsmith and Mason obtained film thicknesses which were about 90% greater. These results demonstrate the divergence between the actual behavior and potential flow theory in the film region, thereby supporting the decision to attempt to modify the theory in this region.

In the model proposed for the flow around a bubble in an actual liquid, the film region can be divided into two distinct sections; one in which a portion of the liquid is accelerating freely and a portion is supported by wall shear and one in which the entire film is in steady laminar flow and supported by wall shear. While the analysis of the flow in the transition region would be rather complex, the analysis of the equilibrium laminar film is relatively straight-forward. This analysis has been carried out in Appendix II.

Before considering the results of the laminar film analysis, however, the applicability of such an analysis to the problem of bubble movement should be determined. The question which arises is whether the results obtained by analyzing the equilibrium film region will be limited to bubbles which have developed this film. Fortunately this is not the case, as experiments[2] have indicated that the velocity of non-expanding Taylor bubbles is independent of bubble length for bubbles ranging in length from one tube diameter to the 'infinite' bubbles formed by draining the liquid from tubes. It should be noted, however, that bubbles rising in a tube open to the atmosphere will indicate an effect of bubble length since the liquid above the bubble will also be rising at a rate determined by the rate of volumetric expansion of the bubble. This effect has been observed experimentally by Laird and Chisholm[6] and by Nicklin[2] and was first explained by Nicklin. For non-expanding bubbles, then, the principles of bubble movement developed from consideration of the equilibrium annular film at the tail of a bubble should apply whether or not this film is present.

The analysis carried out in Appendix II for the equilibrium film flow around a weightless, inviscid bubble leads to the result

$$V_b^o = \frac{\rho g}{\mu} \frac{R^2}{(1-\xi_o)^2}\left[\frac{2}{3}\xi_o^3(1-\xi_o) + \frac{1}{10}\xi_o^5 + \frac{1}{60}\xi_o^6 + \ldots\right] \qquad (9)$$

relating the bubble velocity, $V_b^o$, and the relative thickness of the equilibrium laminar film, $\xi_o = \delta_o/R$. For most of the systems considered in this study, it was possible to neglect all terms of order greater than the fourth and the form of Equation (9) which was used is

$$V_b^o = \frac{2}{3}\frac{\rho g}{\mu} R^2 \frac{\xi_o^3}{(1-\xi_o)} \qquad (10)$$

While the occurrence of laminar flow in the equilibrium film has not been established directly, it has been shown that the film thicknesses which occur are consistent with laminar flow theory. Nicklin[2], in experiments with air bubbles rising through water in a 1.02-in. diameter tube, obtained the film thickness experimentally by collecting the liquid in the film and obtained film thicknesses within 6% of the laminar film thickness predicted by Equation (10). Additional confirmation is provided by White[7] who reports, for a variety of liquids and tube sizes covering a range of film Reynolds numbers ($Re = 2V_b^o\rho(R-\delta_o)^2/R\mu$) from 0.01 to 4000, the result

$$V_b^o = \frac{2}{3}\beta^3 \frac{R^2\rho g}{\mu} \frac{\xi_o^3}{(1-\xi_o)} \qquad (11)$$

where $\beta$ is a factor between 1.05 and 1.11. The assumption of laminar flow in the equilibrium film would not be expected, therefore, to lead to any great errors in the development.

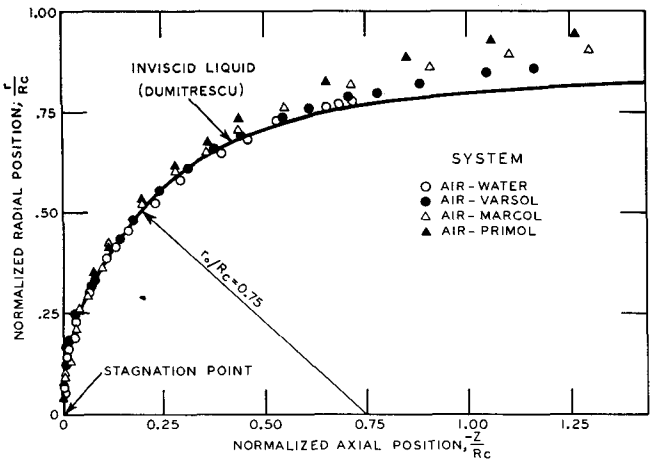


**Figure 3—Normalized bubble shapes.**

**The Nose Region:** As has been noted previously, the theoretical analysis of Dumitrescu for the potential flow at the nose of a Taylor bubble in an inviscid liquid was based on the assumption that the nose was a portion of a spherical surface and determined that the frontal radius was related to the radius of the tube through Equation (4). In connection with the bubble velocity determinations which were summarized in Table 1, bubble shapes were obtained from analysis of photographs of the bubbles to determine the effect on the shape of the liquid viscosity. As was shown in the table, the velocities of air bubbles rising through the liquids were dependent on the liquid viscosity and this effect would be expected to correspond to a change in the shape of the bubble. The experimental equipment and methods used are given in Appendix I.

To compare the geometries of the 'cavities' the experimental bubble shapes were normalized with respect to the equilibrium cylindrical radii, $R_c$, where

$$R_c = R - \delta_o \quad \ldots\ldots (12)$$

and $\delta_o$ was obtained from Equation (10) for the appropriate liquid properties. The normalized coordinates obtained in this manner are $r/R_c$ and $-z/R_c$. The cavity geometries are shown in normalized form in Figure 3. This figure indicates that, although the cavity shapes are different in the transition region, they are remarkably similar in the nose region. The second interesting fact arising from Figure 3 is that the frontal radius of the cavity in normalized coordinates, which is the same for all liquids, is 0.75, the same value as was obtained in the analysis of bubbles in inviscid liquids. Since this implied that a simple correlation of bubble velocities independent of liquid viscosity might result if the equilibrium cylindrical radius was used instead of the tube radius as the characteristic length in the parameter $V_b^o/\sqrt{gR}$, the velocity results were recalculated on this basis. Accordingly, in columns 6 and 7 of Table 1, are given the equilibrium film thicknesses obtained from the experimental bubble velocities with Equation (10) and the corresponding values of the parameter $V_b^o/\sqrt{gR_c}$. The results calculated on this basis do, indeed, indicate a reasonably good correlation with the parameter having the same value as was obtained from the potential flow analysis, namely 0.496. The velocities of Taylor bubbles are well correlated, then, by the equation

$$V_b^o = 0.496\sqrt{gR_c} \quad \ldots\ldots (13)$$

where $R_c$ is the equilibrium cylindrical radius calculable from Equations (10) and (12). The range of applicability of Equation (13) will be considered in a later section.

Before proceeding to apply Equation (13) to further analysis, the significance of the equation will be considered further. The relation actually embodies two independent experimentally observed characteristics of the bubbles. First, the bubble velocity is a unique function of the frontal radius of curvature and is dependent on the liquid viscosity only insofar as the viscosity changes this radius. This unique relation between frontal radius and bubble velocity is similar to the result obtained by Haberman and Morton[8] for large spherical-cap bubbles rising in an infinite liquid medium. For this case, the resulting equation

$$V_b^o = 0.645\sqrt{gr_o} \quad \ldots\ldots (14)$$

was found to apply over a wide range of liquid viscosities.

For comparison with Equation (14), the relation between the frontal radius of curvature and the equilibrium cylindrical radius of the bubble, $r_o = 0.75R_c$, obtained from Figure 3 can be substituted into Equation (13) to give for Taylor bubbles

$$V_b^o = 0.572\sqrt{gr_o} \quad \ldots\ldots (15)$$

Equation (15) differs from the solution for a spherical-cap bubble in an infinite medium (Equation (14)) almost solely due to the different flow situation, the Taylor bubble being enclosed within a tube.

The second characteristic of the bubbles upon which Equation (13) is dependent is the geometrical similarity of the cavities. From the experiments made in this study, it can only be said that the frontal radii are similar relative to the equilibrium cylindrical radii. The present measurements were not corrected for the refraction of light passing through the wall of the tube and near the walls of the tube this effect likely causes considerable distortion. This effect would not distort the frontal radii of curvature, however, as these are measured remote from the walls.

**General Correlation:** Equation (13) relates the bubble velocity to the equilibrium film thickness for a Taylor bubble. It can, therefore, be solved simultaneously with Equation (10) which also relates the film thickness and the bubble velocity. Eliminating the bubble velocity between these two equations results in the following expression for the equilibrium film thickness.

$$\delta_o = \frac{-1 + \sqrt{1 + 2NR}}{N} \quad \ldots\ldots (16)$$

where

$$N = \sqrt[3]{14.5\,\frac{\rho^2 g}{\mu^2}} \quad \ldots\ldots (17)$$

Substituting back into Equation (13) gives the desired expression for the bubble velocity

$$V_b^o = 0.496\sqrt{gR}\sqrt{1 - \frac{-1 + \sqrt{1 + 2NR}}{NR}} \quad \ldots\ldots (18)$$

To recapitulate, Equation (18) has arisen from the experimental observation that Equation (15) describes the velocity behavior of gas bubbles in tubes over a greater range of liquid viscosities than does Equation (3). To use Equation (15), however, it is necessary to know the frontal radius of the bubble and this has been related experimentally to the equilibrium laminar film thickness of the liquid flowing past the bubble on the wall of the tube. A second relation between the bubble velocity and the film thickness results from analysis of the laminar film and the two relations are solved simultaneously for the bubble velocity and the equilibrium laminar film thickness. A final test of the relation will be the comparison of predicted bubble velocities with experimental values from the literature. First, however, the limits of the correlation will be considered.

**Limits of Applicability:** As Equation (18) is being proposed as a general expression for the velocity of rise of a Taylor bubble in a liquid, some consideration must be given to the range of situations to which the equation applies, or, in other words, to the necessary conditions for which a bubble behaves as a Taylor bubble. As was intimated earlier, with increasing

surface tension or with decreasing tube radius the surface tension forces begin to affect the shape of the bubble and it is not longer controlled entirely by the external flow. In this section, an attempt will be made to determine the limit of this surface tension effect or, at least, to determine the pertinent variables for the empirical correlation of the effect.

It was shown earlier that a Taylor bubble rises at a velocity given by the equation

$$V_b^o = 0.572\sqrt{gr_o} \quad \ldots\ldots\ldots\ldots\ldots\ldots\ldots\ldots (15)$$

If, on the other hand, the shape of the bubble nose was determined by the surface tension force, the velocity would be related to the frontal radius by the equation

$$V_b^o = 2\sqrt{\frac{\sigma}{\rho r_o}} \quad \ldots\ldots\ldots\ldots\ldots\ldots\ldots\ldots (19)$$

which is easily derivable from a force balance on an element of the spherical surface assuming that the pressure excess within the bubble due to the surface tension is equal to the stagnation pressure. In Equation (19), $\sigma$ represents the surface tension. It will be noted that the change of velocity with frontal radius is opposite in these two cases, therefore at some radius the velocity obtained from the Taylor bubble hypothesis will also be consistent with the hypothesis of surface tension control. From Equations (15) and (19), the criterion of surface tension control is obtained as

$$0.327\, gr_o > \frac{4\sigma}{\rho r_o} \quad \ldots\ldots\ldots\ldots\ldots\ldots\ldots\ldots (20)$$

which becomes, upon rearrangement,

$$\frac{\rho g r_o^2}{\sigma} > 12.23 \quad \ldots\ldots\ldots\ldots\ldots\ldots\ldots\ldots (21)$$

The dimensionless group $\rho g r_o^2/\sigma$ is a form of the Eötvös number[9]. Substitution into Equation (21) of the relation $r_o = 0.75R_c$, along with Equations (12) and (16), yields the condition

$$\frac{\rho g R^2}{\sigma}\left(1 - \frac{-1 + \sqrt{1 + 2NR}}{NR}\right)^2 > 21.8 \quad \ldots\ldots\ldots\ldots (22)$$

The value of the constant on the right-hand side of Equation (22) is not likely too applicable in view of the approximations made in the development. The equation does, however, indicate the variables which will be likely to affect the onset of surface tension control.

In addition to this limit, which might be termed a surface tension limit, on the applicability of the correlation, there should also be a viscosity limit since for very high liquid viscosities the flow at the nose would be expected to diverge from potential flow. As the analytical solution for this case has not yet been obtained, it is not possible to obtain theoretically this limit on Equation (18) and consideration of it will be deferred until the correlation has been compared with experimental results.

**Comparison with Literature Results:** The dimensionless parameter $2NR$ which arose in the development of Equation (18) is equivalent to the property group used by White and Beardmore[10] to correlate their experimental results for velocities of 'cylindrical' bubbles in the region where the effect of surface tension was negligible. Their correlation extends to $2NR = 113$ and for $2NR > 160$, they recommend the relation

$$\frac{V_b^o}{\sqrt{gR}} = 0.488 \quad \ldots\ldots\ldots\ldots\ldots\ldots\ldots\ldots (23)$$

The relations recommended by White and Beardmore for $2NR > 10$ are shown in Figure 4 as 'dashed' curves while a solid curve has been drawn to show the predictions of Equation (18).

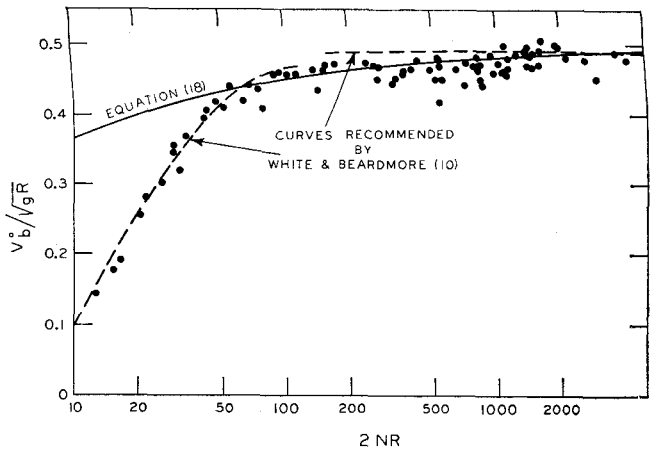


**Figure 4 — Comparison of correlation with experimental results.**

White and Beardmore[10] also considered the limit imposed by increasing surface tension and found empirically that the surface tension effect was negligible for

$$Eo > 17.5 \quad \ldots\ldots\ldots\ldots\ldots\ldots\ldots\ldots (24)$$

where $Eo$ denotes the Eötvös number[9], $Eo = \rho g R^2/\sigma$.

Consideration of experimental results from the literature led to the reformulation of Equation (22) as

$$Eo(1 - \xi_o)^2 > 5.0 \quad \ldots\ldots\ldots\ldots\ldots\ldots\ldots\ldots (25)$$

approximately. This parameter, which includes the effects of surface tension and viscosity, appears to give better correlation to the influence of surface tension than does the Eötvös number alone. The constant 5.0 was obtained by specifying an allowable deviation of about 5% in velocity.

The experimental results shown in Figure 4 are obtained from the literature for tests satisfying condition (25). Table 2 gives a list of the liquids for which experimental bubble velocities in Figure 4 were obtained and the reference to the investigation. Figure 4 indicates that the proposed correlation, Equation (18), describes the experimental results quite well down to a parameter value, $2NR$, of about 60. For parameter values less than about 60, the results are well represented by the correlation of White and Beardmore. This change in behavior is due, presumably, to the change from potential flow to viscous flow at the nose of the bubble, thereby invalidating the assumptions made in deriving Equation (18).

TABLE 2
SOURCE OF EXPERIMENTAL RESULTS

| Liquid | References |
|---|---|
| Water | 1,2,3,4,6,10,11,12,13 |
| Ethanol | 12 |
| Benzene | 12 |
| Ether | 12 |
| Glycol | 10,14 |
| Tellus oil | 10 |
| Voluta oil | 10 |
| Glycerol | 10 |
| Silicone oils | 5 |
| Mineral seal oil | 13 |
| Livestock oil | 13 |
| Carbon tetrachloride | 9 |
| Varsol | 11 |
| Marsol | 11 |
| Primol | 11 |
| Glycerol solutions | 10,14 |
| Sucrose solutions | 10 |
| Butyric acid solutions | 10 |
| Ethanol solution | 10 |
| Sugar syrup solutions | 10 |

The good agreement of the results from the literature with Equation (18) as shown in Figure 4 serves to confirm the model proposed here for the flow around a gas bubble. The limits of applicability of this equation are seen to be:

surface tension:

$$Eo(1 - \xi_o)^2 > 5.0 \quad \ldots\ldots(25)$$

viscosity:

$$2NR > 60 \quad \ldots\ldots(26)$$

**Minimum Size of Taylor Bubbles:** Finally, on the basis of the model proposed here, it is possible to attempt to define the minimum size of bubble in a given system which will exhibit the velocity behavior of a Taylor bubble. Thus, it would be expected that a bubble having an equivalent spherical radius equal to or greater than the frontal radius of a Taylor bubble in the system would rise as a Taylor bubble. In terms of the theory developed here, the size condition for a Taylor bubble can be expressed as

$$r_e > 0.75R\left(1 - \frac{-1 + \sqrt{1 + 2NR}}{NR}\right) \quad \ldots\ldots(27)$$

To check the accuracy of this condition, the results of O'Brien and Gosline[13] and of Uno and Kintner[14] may be considered. In both of these investigations, the effect of bubble size on bubble velocity in various sizes of tubes was obtained experimentally for a number of liquids. Using only those tests for which transition to bubbles rising at constant velocity was observed, this comparison is given in Table 3. The calculated minimum radii are too high in all cases, indicating that transition to Taylor bubble behavior occurs with bubbles of relatively small volume. The bubbles formed in this case are likely spherical-cap bubbles with frontal radii equal to the frontal radii of Taylor bubbles in the tubes. This would account for the discrepancy as the equivalent radii of spherical-cap bubbles are much smaller than the frontal radii.

TABLE 3
MINIMUM SIZES FOR TAYLOR BUBBLES

| Liquid | Tube Radius inches | Equivalent Radius, $r_e$ inches | |
|---|---|---|---|
| | | Calculated[a] | Experimental |
| Water[13][b] | 0.59 | 0.42 | 0.37 |
| | 1.12 | 0.81 | 0.48 |
| Mineral Seal Oil[13] | 0.59 | 0.39 | 0.24 |
| | 1.12 | 0.77 | 0.37 |
| Livestock Oil[13] | 0.59 | 0.35 | 0.32 |
| | 1.12 | 0.71 | 0.38 |
| Glycerine Solution[14] | 0.716 | 0.49 | 0.35 |
| Diethylene Glycol[14] | 0.716 | 0.47 | 0.24 |

[a]Calculated from Equation (27).
[b]Source of experimental results.

## CONCLUSIONS AND DISCUSSION

A model has been proposed for the mechanism of flow associated with the movement of a large gas bubble through stagnant liquid in a tube. This model accounts for the effect of liquid viscosity on the flow in the film around the bubble while retaining the concept of potential flow at the nose which has proven so successful for low viscosity liquids[3]. Experimental observations of bubble geometries indicated that the geometries of the bubbles were similar and this permitted the potential solution for the frontal flow to be linked with the laminar film solution to give the equation

$$V_b^o = 0.496\sqrt{gR}\sqrt{1 - \frac{-1 + \sqrt{1 + 2NR}}{NR}} \quad \ldots\ldots(18)$$

where

$$N = \sqrt[3]{14.5\,\frac{\rho^2 g}{\mu^2}} \quad \ldots\ldots(17)$$

The limits of applicability of Equation (18) were established empirically as

surface tension:

$$\frac{\rho g R^2}{\sigma}\left(1 - \frac{-1 + \sqrt{1 + 2NR}}{NR}\right)^2 > 5.0 \quad \ldots\ldots(25)$$

viscosity:

$$2NR > 60 \quad \ldots\ldots(26)$$

The minimum size of bubble which behaves according to Equation (18) was considered and it was shown that all bubbles which satisfied the condition

$$r_e > 0.75R\left(1 - \frac{-1 + \sqrt{1 + 2NR}}{NR}\right) \quad \ldots\ldots(27)$$

were described by the correlation. The condition was found to be too conservative, however, as smaller bubbles were also described by Equation (18), especially in large diameter tubes.

In this study, the potential flow model for the liquid flow around a large bubble in a tube has been modified to give a better approximation to the physical situation and a better approximation to the bubble behavior. This model also has its shortcomings in that it was not possible to solve for the flow in the transition region and recourse to experiment was necessary. The good agreement of the predictions with experimental results from several sources indicates, however, that the analytical approach has led to an appropriate form of correlation. It is to be hoped that eventually a more complete solution of the flow will be possible and, indeed, a step in this direction has been made by Street[15], who approached the problem of solving for the bubble shape through the integral material and momentum balances and obtained good agreement with the results of Nicklin[2].


### *Acknowledgments*

The author is indebted to G. W. Govier for guidance during the course of the investigation and in the preparation of the manuscript. L. F. Thomas assisted in obtaining the experimental results.

The project was supported financially by the National Research Council of Canada and the author received scholarship assistance from the Government of the Province of Alberta.


## APPENDIX I

### *Experimental Equipment and Procedures*

To supplement the available literature results for rates of rise of air bubbles through liquids in tubes and to obtain some results for the effect of liquid properties on the bubble shape, a series of tests were made. The liquids used comprised water and three petroleum oils, the properties of which have been given in Table 1 in the text. The properties of water have been obtained from standard tables while the densities and viscosities of the three oils were obtained by the Oil and Gas Conservation Board Laboratory of the Government of Alberta. The surface tension values were obtained by the Standards Laboratory of the Department of Chemical and Petroleum Engineering of the University of Alberta in Edmonton.

The cylindrical tube used has been described in the literature[16] and consists of two coupled sections of cellulose-acetate-butyrate tubing to give a length of 37 feet. The tube diameter is 1.038-in. and the wall thickness 0.141-in. The end closures of the tube are full-flow plug valves. Air bubbles were introduced at the lower end of the tube from a reservoir of 1½-in. pipe, the actual introduction being effected by opening the lower plug valve.

As photographs of the bubbles were required to determine the bubble shapes, a one-foot long section of the tube located approximately 25 feet above the lower plug valve was enclosed in a view-box to minimize distortion of the bubble image. The

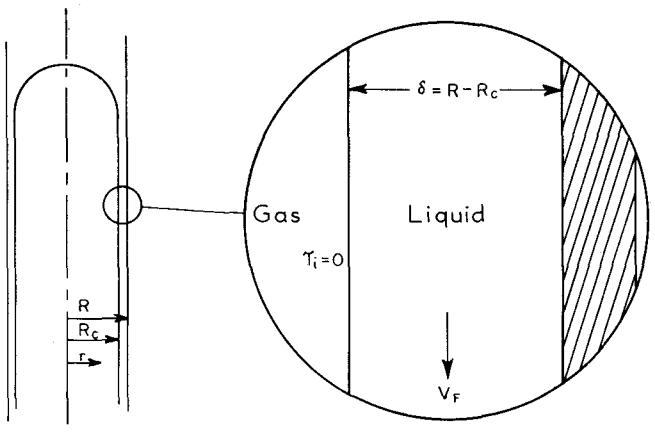


**Figure II-I—The equilibrium film.**

view-box was fabricated from Lucite sheet and fitted onto the tube with O-ring seals. In operation, the view-box was filled with the tube liquid. In the viewing section, the tube was inscribed with several reference lines to aid the quantitative determination of the bubble shape.

Velocity determinations were made in each liquid for a range of bubble sizes. In each case, a measured volume of gas was introduced into the bottom reservoir and pressured to the pressure at the bottom of the liquid column to avoid the sudden disturbance of the liquid column which would take place if the bubble was released without this precaution. The tube was then allowed to sit until liquid motion had stopped and the bubble was released with the lower plug valve.

Bubble velocities were obtained by timing the rise of the bubbles over two successive intervals having lengths of 9.27-ft. and 10.40-ft. respectively. The first timing station was located about thirteen feet above the point of introduction to permit stabilization of the velocities of the bubbles.

For the study of bubble shapes, the bubbles were photographed as they passed through the section of tube enclosed in the view-box. The camera used was an Exacta II equipped with a 50-mm., f-3.5 Tessar lens and it was located about three feet in front of the viewing section, depending on the size of the bubble being measured. The photographs were made with indirect back lighting using two flood lamps to illuminate a white matte board placed behind the viewing section.

The analysis of the bubble shapes was carried out by projecting the image of the bubble nose onto a rear-projection screen with a superimposed arithmetic grid. This procedure and equipment have been described previously[17]. The image was adjusted to remove distortion due to misalignment or anisotropic film shrinkage on the basis of the outer diameter of the tube and the reference lines on the tube. No correction was made to remove optical distortion due to refraction at the tube wall. This distortion is important only for the film region near the tail of a bubble and this region was not sufficiently well defined in these experiments to permit determination of the film thicknesses.

The average velocities obtained in these tests have been given in Table 1 in the text. No effect of bubble length on bubble velocity was found in these tests although bubble lengths ranging from about two inches to ten inches were observed. In addition, there did not appear to be any systematic difference between bubble velocities obtained over the two timing intervals which would indicate that any expansion effect was negligible.

## APPENDIX II

### *Laminar Film Analysis*

Consider the flow of liquid in the annular film shown in section in Figure II-1. For the case being considered here of gas bubbles rising through liquids, the density and viscosity of the gas can be neglected. These assumptions, expressed in terms of the force balance, mean that there is no pressure gradient along the film and that the interfacial shear stress, $\tau_i$, is zero.

The material balance for the flow of liquid relative to the bubble can be written as

$$V_b^o R^2 = (V_b^o + V_F)(R^2 - R_c^2) \quad \text{(II-1)}$$

or

$$V_b^o R_c^2 = V_F(R^2 - R_c^2) \quad \text{(II-2)}$$

where $V_F$ denotes the average liquid velocity in the film relative to the tube wall and $R_c$ is, as before, the equilibrium cylindrical radius of the bubble.

The force balance on an element of film for the assumptions outlined above, and assuming also that the tube is vertical so that the axis of the tube is coincident with the gravity vector, can be given as

$$\frac{1}{r}\frac{\partial(\tau r)}{\partial r} - \frac{\rho g}{g_c} = 0 \quad \text{(II-3)}$$

Integrating Equation (II-3) from the bubble interface gives

$$\tau r = \frac{\rho g}{g_c}\frac{r^2 - R_c^2}{2} \quad \text{(II-4)}$$

If the flow in the film is laminar and the liquid Newtonian, the shear stress can be expressed through the relation

$$\tau = \frac{\mu}{g_c}\frac{du}{dr} \quad \text{(II-5)}$$

which, when substituted into Equation (II-4) and upon integration yields the velocity distribution in the film.

$$-u = \frac{\rho g}{\mu}\left(\frac{R^2 - r^2}{4} - \frac{R_c^2}{2} ln \frac{R}{r}\right) \quad \text{(II-6)}$$

The average velocity of the liquid in the film relative to the wall of the tube can be obtained by integrating the velocity distribution across the film, as shown in the following equation

$$V_F = \frac{2}{R^2 - R_c^2}\int_{R_c}^{R} ur\,dr \quad \text{(II-7)}$$

Substituting Equation (II-6) into Equation (II-7) and integrating gives

$$V_F = \frac{\rho g}{\mu}\left(\frac{R_c^4}{2(R^2 - R_c^2)} ln \frac{R_c}{R} + \frac{3R_c^2}{8} - \frac{R^2}{8}\right) \quad \text{(II-8)}$$

Equation (II-8) can also be expressed in terms of the relative film thickness, $\xi = \delta/R$ where $\delta = R - R_c$.

$$V_F = \frac{\rho g}{\mu}\frac{R^4}{(R^2 - R_c^2)}\left[\frac{2}{3}\xi^3(1-\xi) + \frac{1}{10}\xi^5 + \frac{1}{60}\xi^6 + \ldots\right] \quad \text{(II-9)}$$

Substitution of Equation (II-9) into Equation (II-2) yields the relation between the bubble velocity and the film thickness

$$V_b^o = \frac{\rho g}{\mu}\frac{R^2}{(1-\xi_o)^2}\left[\frac{2}{3}\xi_o^3(1-\xi_o) + \frac{1}{10}\xi_o^5 + \frac{1}{60}\xi_o^6 + \ldots\right] \quad \text{(II-10)}$$

where $\xi_c$ has been used to indicate that the stagnant liquid case is being considered. This result is equivalent to that obtained by Goldsmith and Mason[6].

Manuscript received August 19, 1964; accepted February 15, 1965.
This investigation was carried out as part of a study of vertical, gas-liquid flow in the department of chemical and petroleum engineering, University of Alberta, Edmonton, Alta. Part of this material was presented at the 14th C.I.C. Chemical Engineering Conference, Hamilton, Ont., October 26-28, 1964.

★ ★ ★